Generation of dense spin-wave soliton trains in active ring resonators

Alexey B. Ustinov and Boris A. Kalinikos
Department of Physical Electronics and Technology, St. Petersburg Electrotechnical University, 197376 St. Petersburg, Russia

Vladislav E. Demidov* and Sergej O. Demokritov
Institute for Applied Physics and Center for Nonlinear Science, University of Münster, 48149 Münster, Germany
(Received 15 June 2009; revised manuscript received 11 August 2009; published 28 August 2009)

We have experimentally realized the self-generation of dense trains of spin-wave solitons in active magnetic-film ring resonators. The principle of the soliton auto-oscillator was based on the nonlinear interaction of two copropagating spin waves having the ratio between their group velocities equal to 2 and the transmission bands well separated in the frequency space. We show that under these conditions up to six dark solitons can simultaneously circulate in the active ring. The solitonic nature of the generated pulses is proven by the comparison of the obtained waveforms with those calculated on the basis of the nonlinear Schrödinger equation model.

DOI: 10.1103/PhysRevB.80.052405 PACS number(s): 85.70.Ge, 05.45.Yv, 75.30.Ds, 76.50.+g

Formation and propagation of solitons is one of the most remarkable phenomena in nonlinear physics found in many nonlinear systems of different nature.[1] The basic experimental studies on solitons, as well as their possible technological applications demand the development of auto-oscillators, which can steadily generate solitons with predefined parameters and periodicity. Such systems capable of generation of periodic trains of solitons—soliton lasers, have been widely addressed experimentally and theoretically within nonlinear optics.[2] Nowadays the problem of generation of robust wave packets has also attracted a particular attention in the area of atomic Bose-Einstein condensates.[3,4] Apart from light and matter waves, spin waves propagating in thin ferromagnetic films represent a uniquely flexible model nonlinear system demonstrating solitonic behavior. Since the discovery of spin-wave solitons[5] many interesting solitonic phenomena have been observed in such films, e.g., symmetry-breaking soliton eigenmodes[6] and enhanced interaction of solitons with potential barriers and wells.[7] Note that both these effects have been theoretically predicted for matter waves[8–10] but were experimentally found in magnetic films only.

The problem of the self-generation of spin-wave solitons was addressed experimentally in Refs. 11–13. In particular, the generation of regular sequences of bright and dark solitons,[11,12] as well as the generation of solitons demonstrating fractal temporal patterns[13] was demonstrated in active magnetic-film rings, which are similar in many aspects to optical ring lasers. Contrary to optical soliton lasers, where the effect of soliton energy quantization often resulted in the simultaneous circulation of many solitons inside of the laser cavity,[14] in magnetic-film active rings the mode competition led to a stable self-generation of one or maximum two[15] solitons, which did not allow one to obtain dense soliton trains with high repetition rates.

Here we report on the experimental realization of the self-generation of dense spin-wave soliton trains corresponding to a stable circulation of up to six envelope solitons in the active ring resonator. The self-generation was achieved using the unique controllability of spin-wave dispersion characteristics by the static magnetic field. In particular, varying the angle between the direction of the static magnetization and the film surface we were able to realize the copropagation of two spin waves characterized by the ratio between their group velocities equal to 2. We show that under such experimental conditions the nonlinear interaction between these waves leads to the strong modulational instability resulting in a formation of dense trains of dark spin-wave envelope solitons.

Figure 1 shows the experimental structure of the active ring auto-oscillator. It consisted of a ferromagnetic-film waveguide with lateral dimensions of 2 by 40 mm. It was made from an yttrium iron garnet (YIG) film with the thickness of 13.6 μm. The YIG film had unpinned surface spins, a ferromagnetic resonance linewidth of 0.4 Oe at 5 GHz, and a saturation magnetization $4\pi M_s$ of 1600 G. The output of the waveguide was connected to its input through an active feedback loop consisting of a microwave amplifier and a variable precision attenuator controlling the net gain coefficient G in the ring. The transformation between the electromagnetic wave in the feedback loop and the spin waves propagating in the YIG waveguide was realized by means of two short-circuited 50-μm-wide and 2-mm-long microstrip antennas placed at a distance of 3 mm from each other. The electromagnetic feedback loop played the role of an active part of the ring resonator, whereas its nonlinearity was fully determined by the nonlinearity of the spin system of the YIG

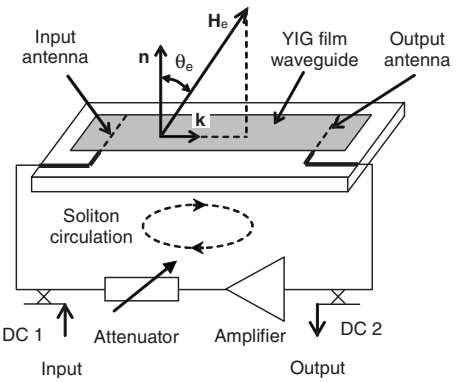

FIG. 1. Diagram of the nonlinear active ring oscillator.

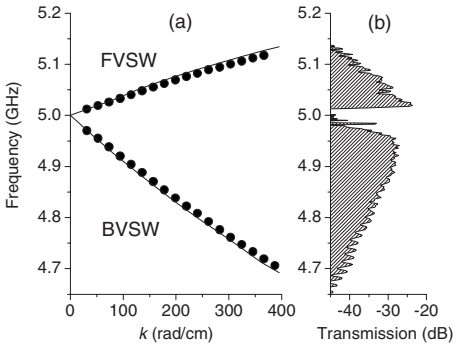

FIG. 2. (a) Dispersion characteristics of spin waves propagating in the YIG waveguide for $\theta_e=34°$. Dots show the experimentally measured data. Lines—results of calculations. $H_e=1929$ Oe. (b) Transmission characteristic of the YIG waveguiding structure measured for the above experimental conditions.

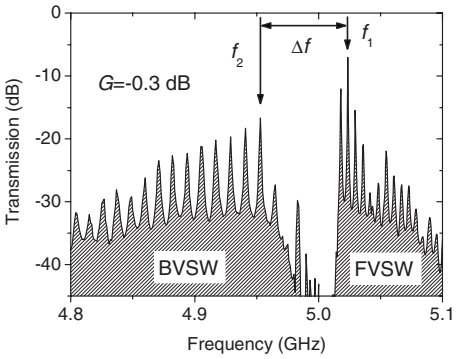

FIG. 3. Transmission characteristic of the ring resonator for the net gain $G=-0.3$ dB. The frequencies f_1 and f_2 correspond to the modes excited as G is increased above the auto-oscillation threshold.

film. Two directional couplers (DC1 and DC2) with the coupling coefficient of −20 dB at the input and the output of the waveguide were used to supply test microwave signals, as well as to couple a small part of the microwave power for monitoring the generated waveforms. A uniform static magnetic field $\mathbf{H}_e$ was applied along the long axis of the YIG waveguide coinciding with the direction of the wave vector of spin waves $\mathbf{k}$. The angle θ_e between the direction of the static magnetic field and the normal to the surface of the film $\mathbf{n}$ was varied in the range from 0° to 90° in order to tune the dispersion characteristics of spin waves.

It is well known[16] that in the above geometry the so-called forward volume spin waves (FVSW) and backward volume spin waves (BVSW) can propagate in the limiting cases of $\theta_e=0°$ and 90°, respectively. These two types of waves have essentially different dispersion. The dispersion curves for both of them start at the frequency of the ferromagnetic resonance at $k=0$ but, with increasing k, the frequency of FVSW increases, whereas the frequency of BVSW decreases. For intermediate angles[17,18] FVSW and BVSW can coexist and, varying θ_e, one can control their group velocities. In fact, in the discussed geometry it is not possible to make the group velocities of the two types of waves to be equal, but for certain values of θ_e the group velocity of BVSW can be a multiple of that of FVSW, which allows a synchronization of their propagation.

In the first step of our experiments we characterized the YIG waveguiding structure and tuned the angle θ_e in order to achieve the above mentioned synchronization. For this we increased the attenuation in the feedback loop to disable it and performed vectorial measurements of the spin-wave transmission characteristics for different θ_e and H_e using the directional couplers DC1 and DC2. The results of these measurements for $\theta_e=34°$ and $H_e=1929$ Oe are presented in Fig. 2. Figure 2(a) shows the dispersion characteristics obtained from the measured phase of the transmission coefficient and Fig. 2(b) presents the modulus of the transmission coefficient. As seen from Fig. 2, for the above combination of θ_e and H_e, the group velocities of FVSW and BVSW, that are proportional to the slopes of the corresponding dispersion curves, differ by a factor of 2. The experimentally measured dispersion characteristics were fitted by theoretical ones calculated using the theory developed in Ref. 17. The results of these calculations are presented in Fig. 2(a) by lines. As seen from the figure, the theoretical curves agree well with the experimental ones with a small mismatch probably caused by the finite width of the YIG waveguide not taken into account in the calculations. Note that, despite the calculated dispersion curves do not show any peculiarities at k approaching to 0, the modulus of the transmission coefficient exhibits a significant decrease at the corresponding frequencies, which leads to a good separation of the FVSW and BVSW bands in the frequency space. The presence of this transmission notch is typical for the studied configuration[17,18] and is, most probably, associated with an inefficient excitation of long-wavelength spin waves by the microstrip antennas.

In the second step we decreased the attenuation in the feedback loop and studied the mode spectrum of the ring resonator as a function of the gain coefficient G. These measurements were performed using a low-power microwave signal supplied to DC1 to preserve the linear response of the system. The critical value of G, at which the auto-oscillation starts, was taken to be equal to 0 dB. Figure 3 shows the modulus of the transmission coefficient measured for $G=-0.3$ dB, i.e., just below the self-generation threshold. Contrary to the case of the disabled feedback, the transmission exhibits a series of narrow peaks corresponding to the linear resonant modes of the ring. Their frequencies are determined by the phase quantization condition $kd+\varphi_e=2\pi n$, where d is the distance between the antennas and φ_e is the phase accumulated by the wave in the feedback loop. Note here, that the term kd, which is equal to the phase accumulated during the propagation in the YIG waveguide, is much larger compared to φ_e. Therefore, the resonant frequencies are determined by the properties of the spin waves rather than by those of the electromagnetic waves in the feedback loop. A simple analysis shows that in this case the frequency spacing between the resonances is determined by the group velocity of the spin waves. In accordance with this conclusion, the observed spacing between the resonant peaks in Fig. 3 is twice larger for BVSW compared to FVSW and equals to 11.8 and 5.9 MHz, respectively.

With increasing G when it exceeds the critical value cor-

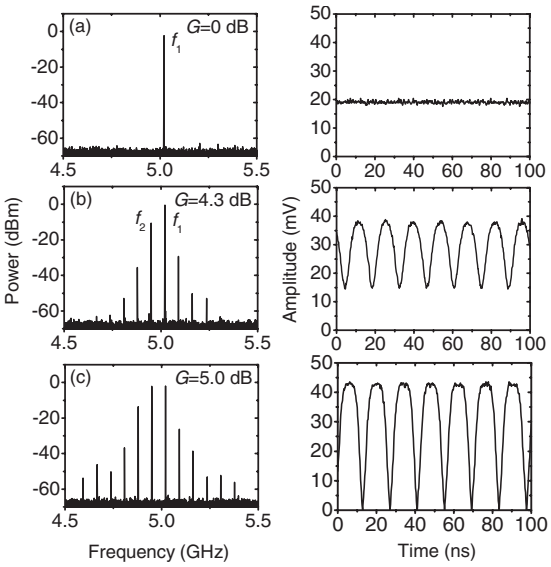

FIG. 4. Power spectra (left column) and waveforms (right column) of the signals generated in the magnetic-film active ring for different values of the gain G, as indicated.

responding to the threshold of the auto-oscillation regime, a resonant mode having the largest gain should be excited. It is seen from Fig. 3 that this condition is met for the mode at the frequency $f_1=5020.5$ MHz situating in the FVSW transmission band. The further increase in G is expected to result in a generation of the second mode characterized by the next largest gain coefficient.[11–13,15] However, due to the mode competition effect this scenario is not necessarily realized in the situation when two waves of different types can propagate in the system. The experiments show that the second mode generated in the studied configuration is always a mode situating in the BVSW band and having the largest gain coefficient among the BVSW modes, i.e., the mode at the frequency $f_2=4949.5$ MHz in Fig. 3. Note that, since the group velocity of BVSW is exactly twice as large as that of FVSW, the frequency spacing between f_1 and f_2 is a multiple of both the frequency separation of BVSW and FVSW modes.

In the third step we studied the auto-oscillation regime of the active ring for the gain above the critical value. These measurements were performed without applying any external signal to the ring. The signals generated by the system were monitored at DC2 by means of a fast microwave diode detector connected to a digital oscilloscope and a microwave spectrum analyzer. Figure 4 presents the key results of these measurements. The right column of Fig. 4 shows the waveforms of the generated signals for different G and the left column shows the corresponding power spectra. As discussed above, at the critical gain $G=0$ dB a monochromatic oscillation appears in the ring at the frequency $f_1=5020.5$ MHz corresponding to the FVSW mode with the largest gain [Fig. 4(a)]. With increasing G the amplitude of the monochromatic signal grows continuously until the second threshold $G=4.3$ dB is reached. At this threshold the largest-gain BVSW mode at $f_2=4949.5$ MHz was excited [Fig. 4(b)]. As soon as two modes were generated in the ring, additional small-amplitude harmonics at combination frequencies appeared in the spectrum. Correspondingly, the waveform in Fig. 4(b) shows a slightly anharmonic oscillation with the frequency $\Delta f=f_1-f_2=71$ MHz. The appearance of the combination frequencies can be associated with a nonlinear interaction of the two waves at frequencies f_1 and f_2 copropagating in the YIG waveguide. Strictly speaking, it is not evident that two waves with significantly different group velocities can demonstrate such an interaction because it appears to be not phase matched. This question was theoretically discussed in numerous papers (see, e.g., Refs. 19 and 20) but only recently it was experimentally shown[21] that this interaction can appear and can result in rather strong modulational instability causing formation of envelope solitons. Since in the studied system Δf is arranged to be multiple of the mode spacing, the frequencies of the nonlinearly generated harmonics coincide with the frequencies of the linear modes of the ring resonator. Therefore, the modulational instability is additionally enhanced by the resonant properties of the system. As seen from Fig. 4(c), further increase in G quickly leads to the development of the instability and the growth of the harmonics in the spectrum. In the time domain this process results in a formation of a sequence of short dark pulses, each one having the shape very close to that of a dark soliton. The stable generation of such sequences was observed for G up to 5.5 dB. Above this value the ring entered a stochastic generation regime.

In order to prove the solitonic nature of the generated dark pulses we applied the nonlinear Schrödinger equation (NLSE) model.[1] Within this model the nonlinear dynamics is considered as interplay between the nonlinear frequency shift and the dispersion characterized by the nonlinear and the dispersion coefficients, respectively. The dispersion coefficients were obtained from the experimental characteristics shown in Fig. 2(a). In particular, the dispersion coefficients for the BVSW measured at the frequency $f_2=4949.5$ MHz and for the FVSW measured at the frequency $f_1=5020.5$ MHz were found to be 1.9×10^3 cm^2 rad/s and 4.2×10^3 cm^2 rad/s, respectively. The nonlinear coefficient was determined from the precise measurements of the shift of the mode frequencies with increasing power of auto-oscillations. For both waves it was found to be 0.1 MHz/mW. Strictly speaking the NLSE model cannot be directly applied to the studied system since two waves with essentially different group velocities and dispersion coefficients participate in the nonlinear interaction. However, if the nonlinear dynamics is mainly determined by the properties of one of these waves, the NLSE model can be used as a theoretical tool. Following this assumption we calculated temporal profiles of NLSE dark solitons using Eq. (4.28) of Ref. 1 for the above coefficients for BVSW and FVSW and compared them with the experimental profiles shown in Fig. 4(c). The results of comparison are presented in Fig. 5. As seen from the figure, for the coefficients of BVSW a very good agreement between the theoretical and experimental profiles of the dark soliton is achieved (note that no fitting parameters were used), whereas for the coefficients of FVSW the theoretical results differ significantly from the experimental ones. This means that, despite the dark solitons were generated as a result of the nonlinear interaction of BVSW and FVSW, their

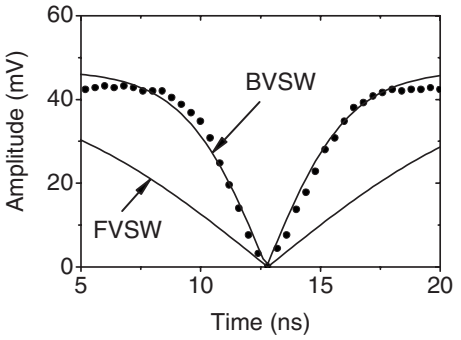

FIG. 5. Points—temporal profile of the dark pulses generated in the active ring. Lines—profiles of a dark soliton calculated taking the experimentally determined parameters of BVSW and FVSW.

characteristics are nearly entirely determined by the group velocity and the dispersion coefficient of BVSW.

Finally, let us analyze the period of the solitons in the generated train [Fig. 4(c)]. In the frequency domain the spectrum of the soliton sequence consists of a number of harmonics at the frequencies of the resonant modes of the ring but the spacing between the harmonics Δf is by a factor of six larger than the spacing between the BVSW modes. In the time domain this corresponds to the fact that the period of the soliton train is by a factor of six shorter than the time needed for a soliton to travel around the ring resonator. In other words, six dark solitons circulate in the ring simultaneously. We emphasize that through varying the length of the YIG waveguide one can efficiently control the frequency spacing between the resonant modes and change the number of solitons circulating in the ring.

In conclusion, we have demonstrated that the tunability of the dispersion characteristics of spin waves owing to the variation in the direction of the static magnetization provides an efficient way for controllable generation of dense soliton trains. The solitons were generated as a result of the nonlinear interaction of two waves with significantly different dispersion properties. Surprisingly, it was found that their characteristics are nearly entirely determined by the parameters of one of the interacting waves. At the moment there is no theory, which could explain these findings but we believe that our results will stimulate theoretical studies in this direction.

This work was supported in part by Russian Foundation for Basic Research under Grant No. 08-02-00959, Russian Federal Agency for Education under Projects No. RNP/2.1.1.371, No. NSh-2124.2008.2, and No. MK-2804.2008.8, and by the Deutsche Forschungsgemeinschaft.

*Corresponding author; demidov@uni-muenster.de

[1] M. Remoissenet, *Waves Called Solitons: Concepts and Experiments* (Springer-Verlag, Berlin, 1996).
[2] Yu. Kivshar and G. Agraval, *Optical Solitons: From Fibers to Photonic Crystals* (Academic, Amsterdam, 2003).
[3] L. D. Carr and J. Brand, Phys. Rev. A **70**, 033607 (2004).
[4] M. I. Rodas-Verde, H. Michinel, and V. M. Pérez-García, Phys. Rev. Lett. **95**, 153903 (2005).
[5] B. A. Kalinikos, N. G. Kovshikov, and A. N. Slavin, JETP Lett. **38**, 413 (1983).
[6] S. O. Demokritov, A. A. Serga, V. E. Demidov, B. Hillebrands, M. P. Kostylev, and B. A. Kalinikos, Nature (London) **426**, 159 (2003).
[7] V. E. Demidov, U.-H. Hansen, and S. O. Demokritov, Phys. Rev. B **78**, 054410 (2008).
[8] L. D. Carr, C. W. Clark, and W. P. Reinhardt, Phys. Rev. A **62**, 063611 (2000).
[9] C. Lee and J. Brand, Europhys. Lett. **73**, 321 (2006).
[10] G. Theocharis, P. Schmelcher, P. G. Kevrekidis, and D. J. Frantzeskakis, Phys. Rev. A **74**, 053614 (2006).
[11] B. A. Kalinikos, N. G. Kovshikov, and C. E. Patton, Phys. Rev. Lett. **80**, 4301 (1998).
[12] B. A. Kalinikos, M. M. Scott, and C. E. Patton, Phys. Rev. Lett. **84**, 4697 (2000).
[13] M. Wu, B. A. Kalinikos, L. D. Carr, and C. E. Patton, Phys. Rev. Lett. **96**, 187202 (2006).
[14] D. Y. Tang, L. M. Zhao, B. Zhao, and A. Q. Liu, Phys. Rev. A **72**, 043816 (2005).
[15] B. A. Kalinikos, N. G. Kovshikov, M. P. Kostylev, and H. Benner, JETP Lett. **76**, 253 (2002).
[16] A. G. Gurevich and G. A. Melkov, *Magnetization Oscillations and Waves* (CRC, New York, 1996).
[17] S. N. Bajpai, R. W. Weinert, and J. D. Adam, J. Appl. Phys. **58**, 990 (1985).
[18] S. N. Dunaev and Y. K. Fetisov, IEEE Trans. Magn. **29**, 3449 (1993).
[19] G. P. Agrawal, Phys. Rev. Lett. **59**, 880 (1987).
[20] M. Yu, C. J. McKinstrie, and G. P. Agrawal, Phys. Rev. E **48**, 2178 (1993).
[21] M. Wu and B. A. Kalinikos, Phys. Rev. Lett. **101**, 027206 (2008).